analytical chemistry

Technical Note

pubs.acs.org/ac

Dual Detection System for Simultaneous Measurement of Intracellular Fluorescent Markers and Cellular Secretion

Lian Yi,[†] Basel Bandak,[†] Xue Wang,[†] Richard Bertram,[‡,§] and Michael G. Roper*[,†,§]

[†]Department of Chemistry and Biochemistry, Florida State University, 95 Chieftain Way, Dittmer Building, Tallahassee, Florida 32306, United States

[‡]Department of Mathematics and Program in Neuroscience, Florida State University, Tallahassee, Florida 32306, United States

[§]Program in Molecular Biophysics, Florida State University, Tallahassee, Florida 32306, United States

Supporting Information

ABSTRACT: Glucose-stimulated insulin secretion from pancreatic β-cells within islets of Langerhans plays a critical role in maintaining glucose homeostasis. Although this process is essential for maintaining euglycemia, the underlying intracellular mechanisms that control it are still unclear. To allow simultaneous correlation between intracellular signal transduction events and extracellular secretion, an analytical system was developed that integrates fluorescence imaging of intracellular probes with high-speed automated insulin immunoassays. As a demonstration of the system, intracellular $[Ca^{2+}]$ ($[Ca^{2+}]_i$) was measured by imaging Fura-2 fluorescence simultaneously with insulin secretion from islets exposed to elevated glucose levels. Both $[Ca^{2+}]_i$ and insulin were oscillatory during application of 10 mM glucose with temporal and quantitative profiles similar to what has been observed elsewhere. In previous work, sinusoidal glucose levels have been used to test the entrainment of islets while monitoring either $[Ca^{2+}]_i$ or insulin levels; using this newly developed system, we show unambiguously that oscillations of both $[Ca^{2+}]_i$ and insulin release are entrained to oscillatory glucose levels and that the temporal correlation of these are maintained throughout the experiment. It is expected that the developed analytical system can be expanded to investigate a number of other intracellular messengers in islets or other stimulus-secretion pathways in different cells.

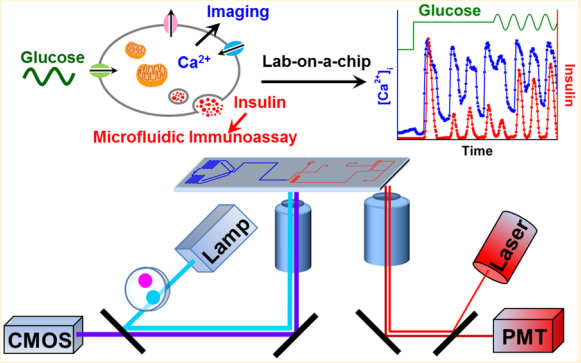

Although the central role of insulin secretion in glucose homeostasis was well established several decades ago, the fundamental mechanisms involved in its control are still incompletely understood. The triggering pathway of glucose stimulated insulin secretion (GSIS) has been well characterized[1,2] and involves production of ATP through metabolism of the sugar leading to closure of K^+_{ATP} channels. In turn, this depolarizes the cell membrane, opening L-type Ca^{2+} channels and producing an increase in intracellular $[Ca^{2+}]$ ($[Ca^{2+}]_i$). As a result, insulin is secreted from the cell. However, this mechanism cannot fully explain all observations of GSIS.[1,2] For example, glucose has been shown to increase insulin secretion independent of its action on K^+_{ATP} channels.[3,4] This pathway, known as the amplifying pathway, does not involve a further increase in $[Ca^{2+}]_i$ but, instead, amplifies the efficacy of the elevated $[Ca^{2+}]_i$ on the exocytosis of insulin granules. Although this pathway has been proposed, the mechanism by which it works remains incompletely identified and is thought to involve secondary messengers generated during glucose metabolism.[1,2,5,6] To better understand the various stimulus-secretion coupling mechanisms that occur during GSIS, it would be ideal to have an automated system that can simultaneously monitor insulin secretion with intracellular messengers at high temporal resolution.

There have been several examples of simultaneous fluorescence imaging of intracellular markers with secretion from β-cells or islets. Most often, $[Ca^{2+}]_i$ is measured with a Ca^{2+}-sensitive fluorescent probe and then combined with a technique that can measure cellular release. For example, simultaneous $[Ca^{2+}]_i$ measurements have been combined with enzyme-linked immunosorbent assays (ELISA) or radioimmunoassays (RIA).[7−9] However, ELISA and RIA are time-consuming and laborious, both of which become exaggerated if high time resolution is required. It would be more ideal if the secretion measurements could be automated and integrated with measurements of intracellular signals.

Recently, microfluidic electrophoretic immunoassays have been used to monitor insulin secretion in an automated fashion with high temporal resolution.[10−14] However, these assays have not been combined with simultaneous measurement of intracellular factors. In this work, a dual fluorescence detection

Received: June 22, 2016
Accepted: October 7, 2016
Published: October 7, 2016

DOI: 10.1021/acs.analchem.6b02404
Anal. Chem. 2016, 88, 10368−10373

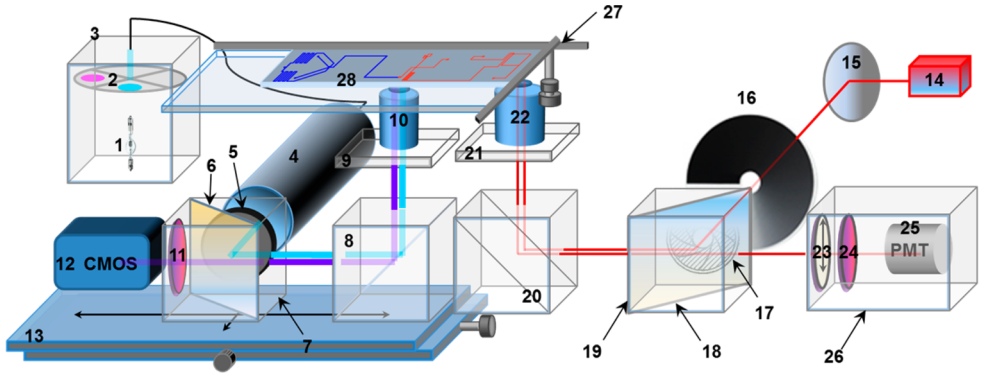

Figure 1. Schematic diagram of the dual detection system. The fluorescence imaging system consisted of: 1, xenon lamp; 2, filter wheel; 3, shutter; 4, collimator; 5, neutral density filter; 6, 409 nm dichroic mirror; 7, dichroic filter cube; 8, dielectric turning mirror; 9, cage plate; 10, 10× objective; 11, 510 ± 84 nm emission filter; 12, CMOS camera; 13, bottom $X-Y$ stage. The LIF detection system consisted of: 14, 635 nm laser; 15, reflective mirror; 16, neutral density filter wheel; 17, graduated iris diaphragm; 18, 405/488/561/635 nm dichroic mirror; 19, dichroic filter cube; 20, dielectric turning mirror; 21, cage plate; 22, 40× objective; 23, linear polarizer; 24, 446/523/600/677 nm emission filter; 25, PMT; 26, photometer. The sample stage consisted of: 27, top $X-Y$ positioner; 28, microfluidic device.

system is described that enables high time resolution imaging of intracellular fluorescent probes simultaneously with measurement of extracellular release. The methodology developed is general and can be expanded to include measurement of other intracellular messengers by changing the fluorescent sensors used. It could also be applied to study the stimulus-secretion coupling of other peptide hormones released from islets or readily applied to other cell types with changes to the assay conditions.

EXPERIMENTAL SECTION

Materials and Experimental Protocol. The materials and reagents, fabrication procedure of the microfluidic device, islet procurement, perfusion system, and data analysis are described in the Supporting Information.

Dual Fluorescence Detection System. The dual fluorescence detection system consisted of a fluorescence imaging system and a laser-induced fluorescence (LIF) system. For fluorescence imaging, a Xenon arc lamp with shutter and filter wheel containing appropriate excitation filters (482 ± 35 nm for fluorescein; 340 ± 5 and 380 ± 5 nm for Fura-2 or Fura-PE3) was used as the excitation source (Lambda XL, Sutter Instruments, Novato, CA). The excitation light was delivered via a liquid light guide to a collimator (CeramOptec, East Longmeadow, MA) and then onto a kinematic dichroic filter cube (Thorlabs, Inc., Newton, NJ). The filter cube had excitation, emission, and dichroic filter slots. For imaging of Fura-2 or Fura-PE3, a 1.0 neutral density filter and a 510 ± 84 nm filter (Semrock, Rochester, NY) were placed in the excitation and emission filter slots, respectively, in combination with a 409 nm dichroic mirror. For fluorescein, a 506 nm dichroic mirror and a 536 ± 40 nm emission filter (Semrock) were used. The excitation light was focused within the islet chamber using a 10×, 0.5 NA infinity-corrected CFI S Fluor objective (Nikon Instruments, Inc., Melville, NY). Emission light was collected with the same objective, passed through the dichroic filter cube and emission filter, and collected with a CMOS camera (QImaging, Surrey, BC, Canada).

For LIF detection of the immunoassay, light from a 100 mW, 635 nm laser (AixiZ, Houston, TX) was passed through a neutral density filter wheel and an iris that were mounted in front of a kinematic dichroic filter cube that held a 405/488/561/635 nm dichroic mirror (Semrock). The light was then directed to the back of a 40×, 0.6 NA objective (Nikon Instruments, Inc.). Emission was collected with the same objective and reflected back through the dichroic cube, spatial filter, 446/523/600/677 nm emission filter (Semrock), and a linear polarizer before being detected by a PMT (Hamamatsu Photonics, Middlesex, NJ). A photometer (Photon Technology International, Inc., Birmingham, NJ) housed the spatial filter, emission filter, polarizer, and PMT.

Fluorescence images were acquired with a 100 ms exposure every 10 s. The timing of the images and Sutter lamp system were controlled by Nikon NIS Elements software (Nikon Instruments, Inc.). The LIF data collection was performed using software written in LabView (National Instruments, Austin, TX).

Insulin Immunoassay Protocol. Microfluidic devices were conditioned daily for 10 min with 1 M NaOH, deionized water, and immunoassay reagents prior to experiments. At the end of the day, the devices were conditioned with deionized water for short-term storage or an additional 1 M NaOH and water for long-term storage. All reservoirs were covered with plastic caps, and electrodes were inserted into the plastic caps for application of voltages.

For all experiments, 150 nM Cy5-labeled insulin (Ins*) and 150 nM monoclonal anti-insulin (Ab) were used in the device and were prepared daily in a buffer containing 25 mM tricine, 1 mM EDTA, and 40 mM NaCl at pH 7.4, supplemented with 1 mg mL^{-1} BSA and 0.1% Tween-20. Gate and waste reservoirs contained 150 mM tricine and 20 mM NaCl with pH adjusted to 7.4. During the experiments, the Ins*, Ab, and islet reservoirs were grounded and −5000 V was applied to the waste reservoir with a high voltage power supply (UltraVolt, Inc., South Thief River Falls, MN). A flow-gated injection scheme was used to inject sample into the separation channel using a high voltage relay (Gigavac, Carpinteria, CA).[15] For calibration curves, 0–1500 nM insulin prepared in balanced salt solution was perfused into the islet reservoir and the ratio of bound (B) and free (F) Ins* (B/F) was monitored. Throughout the text, the concentrations of immunoassay reagents are referred to as the concentration in the fully mixed state, which assumes a 3-fold dilution of the concentrations in the microfluidic reservoirs.

Simultaneous Measurement of $[Ca^{2+}]_i$ and Insulin Secretion. Prior to islet experiments, 2.0 μL of 2.5 mM Fura-2 or Fura-PE3 acetoxymethyl ester in 1:1 (v/v) DMSO/Pluronic

DOI: 10.1021/acs.analchem.6b02404
Anal. Chem. 2016, 88, 10368–10373

F-127 solution was added into 2 mL of RPMI 1640 with 11 mM glucose and L-glutamine. Islets were incubated in this solution for 40 min at 37 °C and 5% CO_2. After this time, islets were loaded into the islet chamber on the microfluidic device with the perfusion flow off. After loading, the perfusion flow was resumed and islets were rinsed with 3 mM glucose for 5 min prior to measurements. The ratio of fluorescence intensities excited at 340 and 380 nm (F340/F380) was converted to $[Ca^{2+}]_i$ using calcium standards (Thermo Fisher Scientific, Inc.). The *B*/*F* from the insulin immunoassay data was analyzed and converted to secretion rate as described in the Supporting Information. To maintain the islet chamber at a physiological temperature and maintain a light path for fluorescence imaging under the islet chamber, two thermofoil heaters (Omega Engineering Inc., Stamford, CT) were taped in parallel under the islet reservoir with a 1 mm gap between the two heaters aligned with the islet chamber. A thermocouple was placed adjacent to the islet reservoir on top of the device, and a controller (Omega Engineering) was used to maintain the temperature in the islet chamber at 36.5 ± 0.5 °C.

RESULTS AND DISCUSSION

In this work, a dual fluorescence detection system was developed that allows simultaneous imaging of intracellular probes with insulin secretion measurements from single islets. Since $[Ca^{2+}]_i$ plays a significant role in GSIS, it was used to demonstrate the ability of the developed system to simultaneously monitor intracellular events with insulin secretion.

Development of a Dual Detection System and Chip Design. A common method for coupling LIF detection for measurement of insulin immunoassays uses inverted fluorescence microscopes.[10−14] To facilitate both detection systems, a dual and inverted fluorescence detection system was constructed using a 30 mm cage assembly (Figure 1).

The microfluidic design previously used for automated insulin immunoassays[13] was modified so that the distance between the islet chamber and LIF detection point approximately matched the distance between the objectives on the dual fluorescence system (~48 × 15 mm). To allow flexibility in the positioning of the microfluidic chip and the location of the excitation sources, the LIF detection system was fixed to the table. A rigid stand insert holder was used to hold the microfluidic system on an *X*−*Y* positioner above the LIF system. This allowed *X*−*Y* movement of the microfluidic device with respect to the LIF system. The 40× LIF objective was mounted onto a *Z*-axis translation stage, which allowed focusing of the laser light into the detection channel of the separation system.

In contrast to the fixed LIF system, the entirety of the fluorescence imaging system was fixed to an *X*−*Y* positioner, allowing translational movement of this system with respect to the islet chamber. A *Z*-axis translational stage was incorporated with the 10× imaging objective to enable focusing of the fluorescence imaging system. A CMOS camera was used to allow spatially resolved imaging, but a PMT could be used if desired.

For experiments, the microfluidic device was first moved using the top *X*−*Y* positioner such that the LIF system was aligned with the detection spot in the separation channel as viewed through the photometer. The fluorescence imaging system was then moved until the islet chamber was in view, at which point the positioning was stopped and the image was focused. To reduce vibrations, blank cage plates and damped posts were used throughout the system.

Characterization of the Microfluidic System. To correlate intracellular events with secretion, glucose was delivered to the islet chamber while $[Ca^{2+}]_i$ was imaged and insulin immunoassays were measured. The microfluidic device design is shown in Figure 2A with the islet chamber indicated

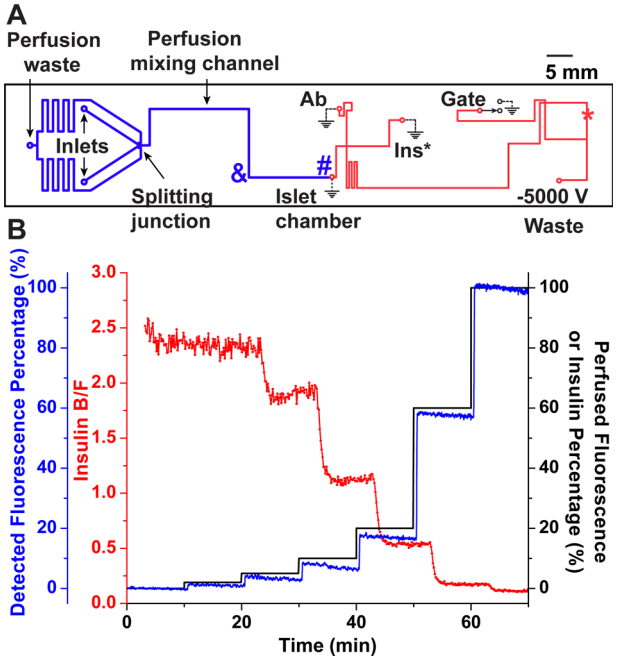

Figure 2. Characterization of the microfluidic system. (A) The channel design of the microfluidic device is shown. The perfusion and electroosmotic flow (EOF) channels are indicated by blue and red lines, respectively. (B) The measured fluorescence (blue) at the corner of the perfusion channel (indicated by &) and measured insulin *B*/*F* (red) when step changes of fluorescein or insulin (right *y*-axis, black) were perfused into the islet chamber.

by the blue # symbol and the LIF detection point indicated by the red ∗ symbol. Due to the difference in locations of these detection points, the times for changes in $[Ca^{2+}]_i$ and insulin had to be correlated. The delay times for each of these points were characterized and used to correct the $[Ca^{2+}]_i$ and insulin secretion profiles.

The perfusion flow rate was calculated by filling one of the syringes in the perfusion system with fluorescein and measuring the time for fluorescein to travel to the corner before the islet chamber (indicated by the blue & symbol in Figure 2A) upon a change in the syringe height. The measured fluorescence intensity is shown in the blue trace in Figure 2B (left *y*-axis), and the step changes in the syringe are shown in the black trace (right *y*-axis). The average delay time of three steps was measured as 33.1 ± 0.4 s, which equated to a volumetric flow rate of 0.21 ± 0.01 μL min^{-1} in the perfusion channel. This flow rate resulted in a delay time of 46.5 ± 0.5 s to the islet chamber, which was used to correct the time delay of the $[Ca^{2+}]_i$ profile. The delay time for each microfluidic device used over the course of the experiments was measured and ranged from 45 to 48 s.

The other delay time was for the insulin system, which included the perfusion delay time in addition to the time required for the secreted insulin to be sampled, mixed with

DOI: 10.1021/acs.analchem.6b02404
Anal. Chem. 2016, 88, 10368−10373

immunoassay reagents, and separated before being detected at the separation detection point. In a similar fashion as described for the perfusion system, step changes of insulin (Figure 2B, black trace, right *y*-axis) were perfused to the islet chamber and the changes in *B*/*F* of the insulin immunoassay were monitored (Figure 2B, red trace, left *y*-axis). As expected, the *B*/*F* decreased for higher concentrations of insulin. The lag time was measured for each device (ranged from 3 to 4 min) and was used to correct all insulin secretion data.

From this trace of insulin perfusion, other system parameters could also be extracted. When insulin concentrations were perfused, the *B*/*F* reached a new plateau in 8 data points (~80 s response time) and stabilized with RSDs ranging from 2% to 5%. The average *B*/*F* was calculated for each insulin concentration, and the resulting calibration curve is shown in Figure S-1. The detection limit was calculated to be 10 nM which enabled the measurement of insulin secretion from single islets at basal and stimulated glucose concentrations.

$[Ca^{2+}]_i$ Imaging and Insulin Secretion. The first test of the dual detection system was to monitor $[Ca^{2+}]_i$ and insulin secretion simultaneously from a single islet under elevated glucose conditions. Figure 3A shows an islet within the islet

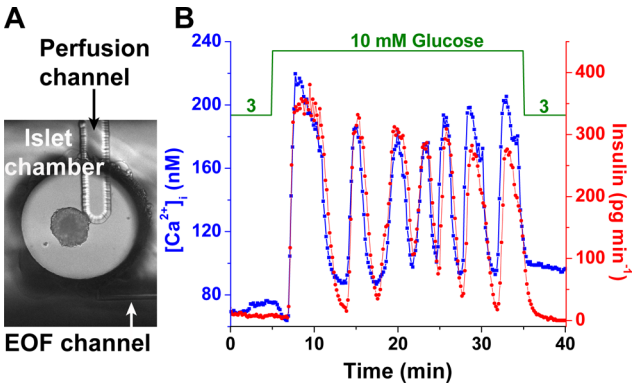

Figure 3. Simultaneous measurement of $[Ca^{2+}]_i$ and insulin secretion from a single islet. (A) Shown is a murine islet of Langerhans situated within the microfluidic device. The perfusion channel was used to deliver glucose to the islet, while the EOF channel was used to sample insulin secretion. (B) The $[Ca^{2+}]_i$ measured from an islet using Fura-2 is shown in blue and corresponds to the left *y*-axis; the insulin secretion rate is shown in red and corresponds to the right *y*-axis, and the delivered glucose concentration is shown in green with the concentrations (in mM) indicated on top.

chamber of the microfluidic device. The perfusion and electroosmotic flow (EOF) channels, used to deliver glucose and to sample insulin, respectively, are highlighted. Figure 3B shows a representative example of the time-corrected $[Ca^{2+}]_i$ and insulin secretion profiles measured from a single islet when a step change of glucose from 3 to 10 mM was delivered. A triphasic response in $[Ca^{2+}]_i$ was observed, consisting of an initial decrease (phase 0), followed by a rapid increase to a sustained elevation (phase 1), and finally regular oscillations (phase 2). Insulin secretion showed a similar pattern with the exception of phase 0, which is likely due to the low $[Ca^{2+}]_i$ during this time. Both $[Ca^{2+}]_i$ and insulin secretion oscillated with similar periods during phase 2.

For most $[Ca^{2+}]_i$ profiles measured with Fura-2, the baseline drifted in time. This phenomenon has been observed previously and attributed to photobleaching or dye loss.[16−19] Use of a more leakage resistant Ca^{2+} dye, Fura-PE3, mitigated this problem and was used for analysis of $[Ca^{2+}]_i$ oscillation peak areas (see below). Regardless of which dye was used, $[Ca^{2+}]_i$ and insulin oscillations from all islets tested (n = 15) exhibited similar oscillation periods as determined by spectral analysis, indicating high temporal correlation. This has been observed previously and suggests that the length and shape of insulin release is determined by the time course of the $[Ca^{2+}]_i$.[1,2] A more rapid $[Ca^{2+}]_i$ image acquisition was possible, but the rate was chosen to match that of insulin measurements. The levels of $[Ca^{2+}]_i$, insulin secretion, and oscillation periods were in agreement with previously reported values.[7,8,11−13,16−20]

Application of Oscillatory Glucose Levels to Islets. In the past, we and others have examined the ability of glucose oscillations to entrain $[Ca^{2+}]_i$ and insulin oscillations.[13,17−21] Entrainment is defined here as the shifting of the period of the $[Ca^{2+}]_i$ or insulin oscillations to the period, or integer multiples of the period, of the external glucose signal. In most cases, these experiments have been used to test the hypothesis that an in vivo negative feedback loop may be responsible for synchronizing insulin secretion from multiple islets in the pancreas.[13,17,18,20,21] In these experiments, either $[Ca^{2+}]_i$ or insulin was measured, but never simultaneously, leading to a lack of direct evidence for simultaneous entrainment. To study their correlation directly, we applied small amplitude glucose oscillations to single islets and used the dual detection system to monitor $[Ca^{2+}]_i$ and insulin secretion simultaneously.

Figure 4A details an experimental procedure where the glucose concentration was increased from 3 to 10 mM for 25 min, inducing $[Ca^{2+}]_i$ and insulin oscillations. At 30 min, the glucose concentration was made to oscillate with an amplitude of 2 mM and a period of 5 min. After 20 min, the phase of the glucose oscillations was shifted 180° in an attempt to disrupt the entrainment if it existed. To determine if the islets were entrained, the phase angles between each oscillation of $[Ca^{2+}]_i$ (blue) or insulin (red) and glucose was measured (Figure 4B) as described in the Supporting Information.[13,17,20] Entrainment is indicated by the phase angles converging to a similar value. Typically, if the spread is <45°, it indicates entrainment.[13,17,20] As shown in Figure 4B, during the initial period of glucose oscillations (blue and red squares), the angles converged within a ~30° spread. After application of the phase shift (blue and red triangles), the phase angles again converged to a small spread, with the exception of the first two oscillations (labeled as 1 and 2 in Figure 4B), which has also been noted in past reports.[17,20] The results of all tested islets (n = 8) showed that, upon application of glucose sinusoidal waves, both $[Ca^{2+}]_i$ and insulin were entrained to the forcing period of sinusoidal glucose wave with amplitudes of 2 and 1 mM. This is a direct demonstration that $[Ca^{2+}]_i$ and insulin oscillations maintain their temporal relationship during exposure to oscillatory glucose levels.

As seen in Figure 4A, during the oscillatory glucose delivery, the amplitude of the insulin levels increased whereas those of $[Ca^{2+}]_i$ did not. This effect was observed in 7/8 islets that were entrained to oscillatory glucose levels. Elevated insulin levels without a corresponding increase in the amplitude of $[Ca^{2+}]_i$ oscillations have been observed before and were attributed to the amplifying pathway of GSIS,[1,2,8,9] where metabolic intermediates produced during glucose metabolism increase the efficacy of the raised $[Ca^{2+}]_i$ on insulin release without a further increase in the $[Ca^{2+}]_i$ amplitude. We could not confirm an increase in $[Ca^{2+}]_i$ peak area due to the rising baseline when using Fura-2. By using Fura-PE3, the baseline was more constant and 3/3 islets showed corresponding increases in

DOI: 10.1021/acs.analchem.6b02404
Anal. Chem. 2016, 88, 10368−10373

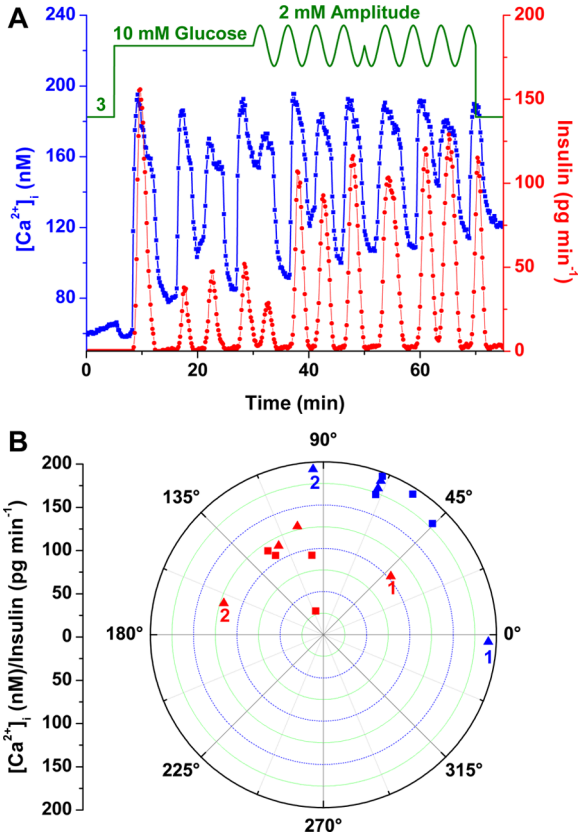

Figure 4. Analysis of $[Ca^{2+}]_i$ and insulin levels during oscillatory glucose exposure. (A) Glucose was raised from 3 to 10 mM to induce $[Ca^{2+}]_i$ oscillations (blue) and insulin secretion (red) from a single islet. The glucose concentration was then oscillated with a period of 5 min and amplitude of 2 mM. A 180° phase shift to the glucose levels was introduced at 50 min. (B) The amplitudes of $[Ca^{2+}]_i$ (red) and insulin (blue) oscillations plotted against their respective phase angles before (■) and after the 180° phase shift (▲). The data points labeled "1" and "2" correspond to the 1st and 2nd measured phase angles after the 180° phase shift.

$[Ca^{2+}]_i$ oscillation peak area but not the height, during exposure to oscillatory glucose levels (see Figure S-2 for an example).

As mentioned, this lack of correlation between $[Ca^{2+}]_i$ and insulin peak amplitudes is attributed to the amplifying pathway of GSIS. In the results shown here, the average extracellular glucose level remains constant with only the instantaneous glucose level changing. This points to a potentially significant role for small amplitude glucose oscillations in vivo amplifying insulin release from the pancreas.

CONCLUSION

A dual detection system consisting of fluorescence imaging and LIF detection was developed to simultaneously monitor intracellular events and extracellular secretion from single islets of Langerhans. Although $[Ca^{2+}]_i$ is shown here, the method is applicable to other intracellular messengers involved in GSIS using different fluorescent probes. For example, different fluorescent sensors have been used to measure the activity of pyruvate kinase,[22] cyclic AMP,[23] the ATP/ADP ratio,[24] and mitochondrial membrane potential.[19] Since stimulus-secretion coupling involves multiple messengers and interactions between these messengers, a system that has the ability to measure several of these simultaneously with insulin secretion is expected to be a valuable tool in the study of GSIS. Also, with changes to the immunoassay reagents, the developed system can be applied to study stimulus-secretion coupling from other cell types.

ASSOCIATED CONTENT

Supporting Information

The Supporting Information is available free of charge on the ACS Publications website at DOI: 10.1021/acs.analchem.6b02404.

Materials, fabrication of the microfluidic device, isolation and culture of islets of Langerhans, detailed info on the perfusion system and data analysis, a calibration curve for insulin, and a trace of simultaneous insulin and Ca^{2+} measurements using Fura-PE3 (PDF)

AUTHOR INFORMATION

Corresponding Author

*Phone: 850-644-1846. Fax: 850-644-8281. E-mail: roper@chem.fsu.edu.

Author Contributions

The manuscript was written through contributions of all authors. All authors have given approval to the final version of the manuscript.

Notes

The authors declare no competing financial interest.

ACKNOWLEDGMENTS

We would like to thank Professor Les Satin for suggesting the use of Fura-PE3. This work was supported by a grant from the National Institutes of Health (R01 DK080714).

REFERENCES

(1) Henquin, J. C. *Diabetologia* **2009**, *52*, 739−751.
(2) Henquin, J. C. *Diabetes Res. Clin. Pract.* **2011**, *93*, S27−31.
(3) Gembal, M.; Detimary, P.; Gilon, P.; Gao, Z. Y.; Henquin, J. C. *J. Clin. Invest.* **1993**, *91*, 871−880.
(4) Sato, Y.; Anello, M.; Henquin, J. C. *Endocrinology* **1999**, *140*, 2252−2257.
(5) Jensen, M. V.; Joseph, J. W.; Ronnebaum, S. M.; Burgess, S. C.; Sherry, A. D.; Newgard, C. B. *Am. J. Physiol. Endocrinol. Metab.* **2008**, *295*, E1287−1297.
(6) Maechler, P.; Carobbio, S.; Rubi, B. *Int. J. Biochem. Cell Biol.* **2006**, *38*, 696−709.
(7) Gilon, P.; Shepherd, R. M.; Henquin, J. C. *J. Biol. Chem.* **1993**, *268*, 22265−22268.
(8) Gilon, P.; Henquin, J. C. *Endocrinology* **1995**, *136*, 5725−5730.
(9) Ravier, M. A.; Henquin, J. C. *FEBS Lett.* **2002**, *530*, 215−219.
(10) Roper, M. G.; Shackman, J. G.; Dahlgren, G. M.; Kennedy, R. T. *Anal. Chem.* **2003**, *75*, 4711−4717.
(11) Shackman, J. G.; Dahlgren, G. M.; Peters, J. L.; Kennedy, R. T. *Lab Chip* **2005**, *5*, 56−63.
(12) Dishinger, J. F.; Reid, K. R.; Kennedy, R. T. *Anal. Chem.* **2009**, *81*, 3119−3127.
(13) Yi, L.; Wang, X.; Dhumpa, R.; Schrell, A. M.; Mukhitov, N.; Roper, M. G. *Lab Chip* **2015**, *15*, 823−832.
(14) Lomasney, A. R.; Yi, L.; Roper, M. G. *Anal. Chem.* **2013**, *85*, 7919−7925.
(15) Jacobson, S. C.; Ermakov, S. V.; Ramsey, J. M. *Anal. Chem.* **1999**, *71*, 3273−3276.
(16) Luciani, D. S.; Misler, S.; Polonsky, K. S. *J. Physiol.* **2006**, *572*, 379−392.
(17) Zhang, X.; Grimley, A.; Bertram, R.; Roper, M. G. *Anal. Chem.* **2010**, *82*, 6704−6711.

DOI: 10.1021/acs.analchem.6b02404
Anal. Chem. 2016, 88, 10368−10373

(18) Zhang, X.; Daou, A.; Truong, T. M.; Bertram, R.; Roper, M. G. *Am. J. Physiol. Endocrinol. Metab.* **2011**, *301*, E742−747.
(19) Pedersen, M. G.; Mosekilde, E.; Polonsky, K. S.; Luciani, D. S. *Biophys. J.* **2013**, *105*, 29−39.
(20) Dhumpa, R.; Truong, T. M.; Wang, X.; Bertram, R.; Roper, M. G. *Biophys. J.* **2014**, *106*, 2275−2282.
(21) Chou, H. F.; Ipp, E. *Diabetes* **1990**, *39*, 112−117.
(22) Merrins, M. J.; Van Dyke, A. R.; Mapp, A. K.; Rizzo, M. A.; Satin, L. S. *J. Biol. Chem.* **2013**, *288*, 33312−33322.
(23) Dyachok, O.; Isakov, Y.; Sagetorp, J.; Tengholm, A. *Nature* **2006**, *439*, 349−352.
(24) Li, J.; Shuai, H. Y.; Gylfe, E.; Tengholm, A. *Diabetologia* **2013**, *56*, 1577−1586.

DOI: 10.1021/acs.analchem.6b02404
Anal. Chem. 2016, 88, 10368−10373